Check for updates

Phenacyl bromide as Norrish type I photoinitiator for the facile synthesis of chain-end functional PMMA and polystyrene

Mina Kati, Yusra Bahar Cakir, Kerem Kaya,
Huseyin Cem Kiliclar* and Baris Kiskan*

Department of Chemistry Maslak, Faculty of Science, Istanbul Technical University, Istanbul, Türkiye

Phenacyl bromide has been explored as a new Norrish Type I photoinitiator for radically polymerizing methyl methacrylate and styrene monomers. A straightforward radical photopolymerization method using UVA light for the synthesis of chain-end functional poly(methyl methacrylate) and polystyrene has been developed. The process has been refined for both bulk and solution photopolymerizations. Chain-end functionalization was demonstrated by the formation of block-copolymers of the bromine-ended homopolymers, utilized as macroinitiators, resulting in an increase in the molecular weight of the corresponding precursor, observed by gel permeation chromatography (GPC). Block copolymerization was initiated by radicals generated at the chain-ends by a halogen-atom transfer reagent, namely, dimanganese decacarbonyl $(Mn_2(CO)_{10})$. This simple light-induced method is promising for the additive manufacturing field such as vat photopolymerization, stereolithography, digital light processing as it yields chain-end functional materials that can be further processed.

KEYWORDS

free radical photopolymerization, Norrish type I photoinitiator, phenacyl bromide, chainend functionalization, halogen abstraction, block copolymerization

1 Introduction

Photochemistry has gained significant attention recently due to the growing emphasis on sustainability and spatiotemporal control in commercial systems (Albini and Fagnoni, 2004; Clark, 2006; Crivello and Reichmanis, 2014; Kaya et al., 2023). The precise and effective energy transfer facilitated by light within a defined space enables green synthesis with temporal control (Lalevée and Fouassier, 2015; Lalevée et al., 2015; Corrigan et al., 2019). These advantages have been utilized in commercialized additive manufacturing (AM) and lithography techniques, employing various photochemical reactions to produce previously unimaginable products (Ober et al., 2019; Ober et al., 2023; Zhang et al., 2019;

Abbreviations: GPC, Gel Permeation Chromatography; NMR, Nuclear Magnetic Resonance; ATRP, Atom-Transfer Radical Polymerization; PAB, Phenacylbromide; RAFT, Reversible Addition-Fragmentation-Chain-Transfer; TPO, Diphenyl(2,4,6-trimethylbenzoyl) phosphine oxide; MMA, Methyl Methacrylate; PS, Poylstyrene; PMMA, Poly(methyl methacrylate); TEGDMA, Triethylene glycol dimethacrylate; DSC, Differential Scanning Calorimetry; FTIR, Fourier-Transform Infrared.

GRAPHICAL ABSTRACT
Table of Contents (TOC).
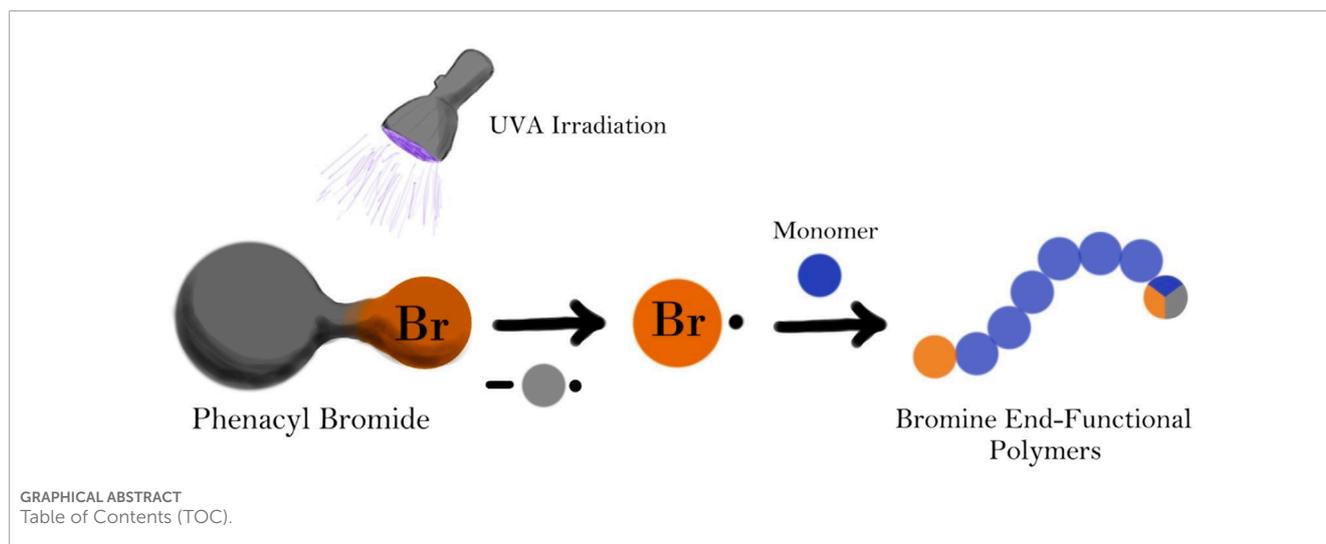
Petko et al., 2021; Petko et al., 2022; Tomal et al., 2021; Bobrin et al., 2022). This rapid development also triggered the quest for better performing photoinitiators to maintain pace with advancing technologies. Beyond effective initiation, novel initiators are also expected to offer features such as chain-end functionalization. Readily substitutable functionalities at the chain ends can be further exploited to finely tune the properties like chain association, hydrophilicity, solubility, surface characteristics and rheology of the polymer (Pispas and Hadjichristidis, 1994; Zha et al., 2016; Ishiwari et al., 2018; Mohammad et al., 2021a; Mohammad et al., 2021b). Moreover, these functionalities can be utilized in synthesizing blocks, grafts and hyperbranched polymers to meet specific needs across various fields (Yagci and Tasdelen, 2006; Aydogan et al., 2017; Mohammad et al., 2021a; Kiliclar et al., 2022; Kumar et al., 2022; Cakir et al., 2023). Therefore, developing a facile method to achieve these functionalities is of great importance. Traditionally, techniques like atom transfer radical polymerization (ATRP), reversible addition-fragmentation chain transfer (RAFT), photoinduced radical oxidation- addition-deactivation (PROAD) and iniferter methods have been frequently used for the synthesis of chain-end functionalized polymers (Matyjaszewski et al., 1998; Otsu, 2000; Matyjaszewski and Xia, 2001; Gody et al., 2015; Ciftci and Yagci, 2018; Dworakowska et al., 2022). However, these methods often rely on either heat or air/moisture sensitive catalysts (Cu catalyst) which require special treatment (freeze-pump-thaw) making them challenging techniques for large-scale processes (Allushi et al., 2017; Ciftci and Yagci, 2018).

Conventional Norrish Type I photoinitiators e.g., benzoin, acylphosphine oxide and acylgermanes were being used in several applications including coatings, dentistry, inks and additive manufacturing (Yagci et al., 2010; Kowalska et al., 2021; Tomal et al., 2022; Buchon et al., 2023). Despite their wide utility, classical Type I photoinitiators cannot produce chain-end functional polymers, which limits their potential for broader applications. Alternatives that enable chain-end functionalization can be crucial for specific purposes, as photochemically generated species can be covalently bonded at the chain-end during the initiation step. Previously bromine (Br_2) has been directly utilized as a photoinitiator for radical polymerization to yield chain-end functional polymers (Ghosh et al., 1973). However, its high toxicity and oxidative nature makes the process inconvenient for large scale use.

This work proposes the novel use of phenacyl bromide (PAB) as a Type I photoinitiator, producing polystyrene (PS) and poly(methyl methacrylate) (PMMA) under UVA light via *in-situ* bromine radical generation. The existence of chain-end bromine functionality was used to create radicals by using $Mn_2(CO)_{10}$ as halogen-atom transfer reagent. The formed radicals by abstraction of bromine were capable to initiate free radical polymerization, enabling the synthesis of a variety of copolymers.

2 Materials and methods

2.1 Materials

Methyl methacrylate (MMA; Merck, 99%) and styrene (St, Merck, 99%) were used after filtration through basic alumina to remove the inhibitor and then stored in the fridge. Dichloromethane (DCM; Sigma-Aldrich %99.8) was purified from amylene stabilizer prior to use. 2-bromoacetophenone (phenacyl bromide) (PAB, Sigma-Aldrich, >98%), dimanganase decacarbonyl (Merck, 98%), *n*-hexane (Sigma-Aldrich, 98%), and methanol (MeOH, Sigma-Aldrich, ≥99.9%) were used as received.

2.2 Methods

2.2.1 Synthesis of poly(methyl methacrylate) (PMMA)

Poly(methyl methacrylate) (PMMA) was synthesized via free radical photo polymerization, conducted either in bulk or with the use of a solvent.

2.2.1.1 Bulk polymerization conditions

2 mL of methyl methacrylate (18.78 mmol) and 20 mg of phenacyl bromide (PAB) (0.10 mmol) were introduced into a dry

reaction flask which was then purged with dry nitrogen gas to create an inert atmosphere. The reaction flask containing the reaction mixture was exposed to irradiation using a photoreactor equipped with 18 Philips TL-36W BLB lamps. These lamps emitted light at a nominal wavelength of 365 nm with an intensity of *ca*. 100 mW·cm^2. After the irradiation, the resulting polymer was precipitated in *n*-hexane and then dried under reduced pressure.

2.2.1.2 Solution polymerization conditions

2 mL of methyl methacrylate (18.78 mmol), 20 mg of PAB (0.10 mmol) and 2 mL of DCM were introduced into a dry screw-capped reaction flask, which was then purged with dry nitrogen gas to create an inert atmosphere. The reaction flask containing the reaction mixture was exposed to irradiation using a photoreactor equipped with 18 Philips TL-36W BLB lamps. These lamps emitted light at a nominal wavelength of 365 nm with an intensity of *ca*. 100 mW·cm^2. After the irradiation, the resulting polymer was precipitated in *n*-hexane and then dried under reduced pressure.

2.2.2 Synthesis of polystyrene (PS)

2.2.2.1 Bulk polymerization conditions

Polystyrene (PS) was synthesized through free radical polymerization using procedures analogous to those used for the synthesis of PMMA. 2 mL (17.46 mmol) of styrene and 20 mg (0.10 mmol) of PAB were combined in a dry screw-cabbed reaction flask under the nitrogen environment. The reaction mixture was exposed to irradiation using a photoreactor equipped with 18 Philips TL-36W BLB lamps. These lamps emitted light at a nominal wavelength of 365 nm with an intensity of approximately 100 mW·cm^2. The obtained mixture was precipitated in methanol and dried under low pressure.

2.2.2.2 Solution polymerization conditions

2 mL of DCM, 2 mL (17.46 mmol) of styrene and 20 mg (0.10 mmol) of PAB were combined in a dry screw-cabbed reaction flask under the nitrogen environment. The reaction mixture was exposed to irradiation using a photoreactor equipped with 18 Philips TL-36W BLB lamps. These lamps emitted light at a nominal wavelength of 365 nm with an intensity of approximately 100 mW·cm^2. The obtained mixture was precipitated in methanol and dried under low pressure.

2.2.3 Copolymer synthesis

2.2.3.1 Synthesis of poly(MMA-*co*-styrene) via PMMA macroinitiator

The reaction flask was equipped with a magnetic stirrer and heated *in vacuo* with the heat gun. When the tube cooled down, it was charged with PMMA macroinitiator (97.5 mg, 0.01 mmol), dichloromethane (2 mL, 31.20 mmol), styrene (2 mL, 17.46 mmol) and dimanganese decacarbonyl (35.6 mg, 0.09 mmol). Following the process of nitrogen purging, the sample is subsequently exposed to a 400 nm UV light for 4 h. After irradiation, the resulting polymer was precipitated in *n*-hexane. Then it is dried under reduced pressure.

2.2.3.2 Synthesis of poly(styrene-*co*-MMA) via PS macroinitiator

67 mg (0.02 mmol) of PS and 14 mg (0.04 mmol) of dimanganese decacarbonyl were dissolved in MMA in a reaction flask with a magnetic stirrer under a dry nitrogen atmosphere. Then the mixture is placed under a 400 nm UV light for 4 h. The obtained polymer was dissolved in methanol and dried under reduced pressure.

2.2.4 Characterization methods

2.2.4.1 Photo-DSC procedure

10 mg (~35 mmol) of TEGDMA together with either 0.01 molar equivalent of PAB or 0.01 molar equivalent of TPO was dropped inside a Photo-DSC pan using a 10 μL micropipette. Then, the pan was irradiated under nitrogen atmosphere using 320–500 nm light source at constant temperature (30°C) until the polymerization was completed (ca. 10 min). The conversion (C) was calculated by using the formula $C = \Delta_{Ht}/\Delta_{H0}$, where Δ_{Ht} is the reaction heat evolved at time t and Δ_{H0} is the theoretical heat for complete conversion. Δ_{H0} for TEGDMA is 81.40 kJ mol^{-1} (Anseth et al., 1994b; Anseth et al., 1994a; Andrzejewska and Andrzejewski, 1998; Dickens et al., 2003).

2.2.4.2 Gel permeation chromatography

Gel permeation chromatography (GPC) analyses were run on TOSOH EcoSEC GPC system equipped with an autosampler system, a temperature-controlled pump, a column oven, a refractive index (RI) detector, a purge and degasser unit, and a TSK gel superhZ 2000 4.6 mm ID × 15 cm × 2 cm column. 1.0 mL min^{-1} of tetrahydrofuran was utilized as the eluent at a temperature of 40°C. Calibrations were done by polystyrene standards with a narrow and limited molecular weight distribution. The data were analyzed by Eco-SEC analysis software.

2.2.4.3 Nuclear magnetic resonance spectroscopy

H-NMR spectra were recorded on an Agilent VNMRS 500 NMR spectrometer system at room temperature in CDCl$_3$ with Si(CH$_3$)$_4$ as an internal standard.

2.2.4.4 Infrared spectroscopy

The Fourier-transform infrared (FTIR) spectroscopy measurements were recorded as 16 scans using a PerkinElmer FTIR Spectrum One spectrometer.

3 Results and discussion

Phenacyl bromide (PAB) has been previously demonstrated to undergo homolytic cleavage of its carbon-bromine covalent bond when exposed to UVA irradiation (McGimpsey and Scaiano, 1988). This process generates bromine radicals together with relatively less reactive carbon-centered radicals. While both radicals have the capability to initiate radical polymerization, bromine radicals are likely to dominate the initiation step, resulting in polymer with bromine chain-end functionality (Scheme 1A). Bromine atom bonded to sp^3 hybridized carbon located at the ß-position of the initial monomer unit offers versatile post-polymerization modification opportunities. It can undergo nucleophilic substitution reactions (Scheme 1B) or be abstracted by halogen-atom transfer techniques such as dimanganese decacarbonyl (Mn$_2$(CO)$_{10}$) chemistry (Scheme 1C) (Arslan et al., 2022). Generated radicals can be further exploited for the synthesis of more complex polymer architectures such as block, graft and hyperbranched copolymers (Scheme 1D).
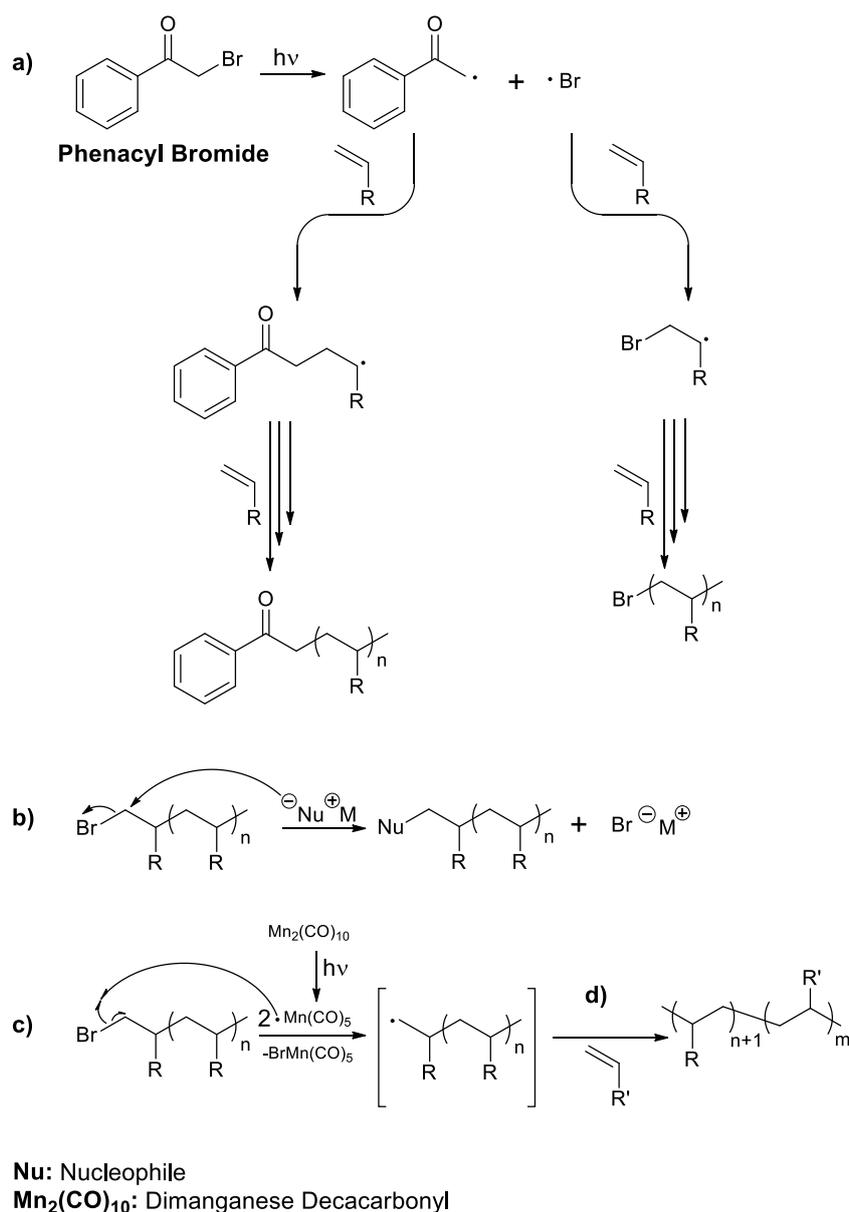
SCHEME 1
(A) Photoinduced radical polymerization of vinyl monomers using PAB as Type I photoinitiator. **(B)** S_N2 type substitution reaction between bromine bonded to sp³ hybridized carbon and a nucleophile. **(C)** Halogen abstraction by photochemically generated $Mn(CO)_5$ radicals from the polymer chain-end. **(D)** Synthesis of block copolymers through chain-end activation.

The ability to easily modify the polymer chain ends opens up numerous possibilities for tailoring polymers obtained from phenacyl bromide initiators. Hence, we displayed this versatility by using classical MMA and Styrene (S) monomers. Initially, to establish optimal photopolymerization conditions, reactions were conducted using both solution and bulk polymerization methods. Reactions were monitored for 6 h or until vitrification occurred. For solution polymerizations, dichloromethane (DCM) and ethyl acetate were selected as solvents due to their compatibility with the monomers and initiator. Moreover, these solvents also offer good transparency in the UVA region, ensuring efficient light penetration throughout the reaction mixture. The

polymerization details and molecular weight characteristics of the obtained polymers were carefully analyzed. Figure 1 illustrates the progression of these reactions over time, showing the evolution of molecular weight. Table 1 provides a comprehensive overview of the reaction conditions and the resulting polymer properties, including number-average molecular weight (M_n), weight-average molecular weight (M_w), and dispersity index ($Đ$).

Bulk polymerization results, as shown in Figure 1, reveal that vitrification occurs rapidly for MMA, taking only 15 min, while styrene requires 6 h. However, solution polymerization offers more precise control over molecular weight and yields more consistent results by eliminating the vitrification. Gel permeation
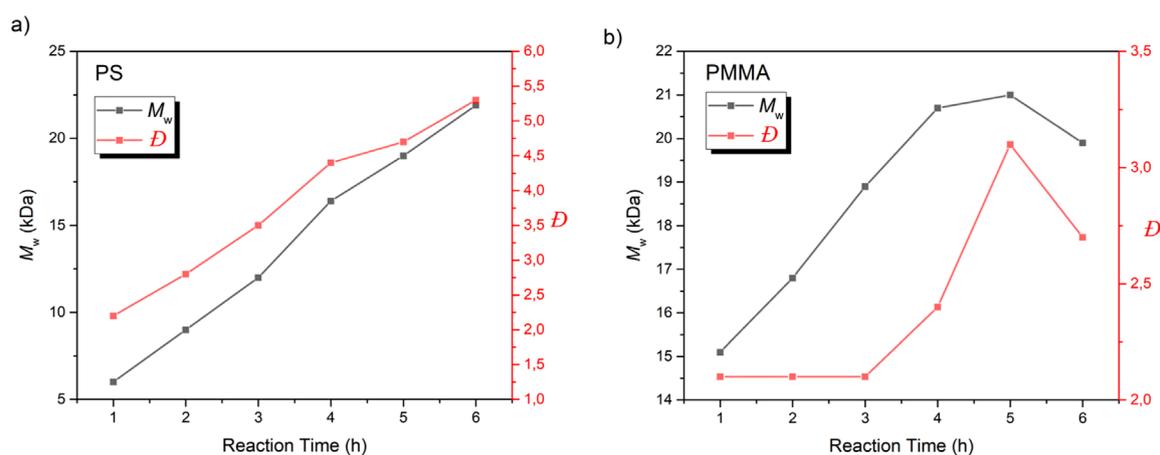
FIGURE 1
M_w versus reaction time graph of **(A)** S and **(B)** MMA polymerization using PAB as photoinitiator.

TABLE 1 Photoinitiated FRP of MMA and styrene monomers using PAB as Type I photoinitiator.

Polymer	Reaction time (h)	M_w^d (kg·mol^{-1})	M_n^d (kg·mol^{-1})	$Đ^d$
PMMA[a]	1	15.1	7.2	2.1
PMMA[a]	2	16.8	8.0	2.1
PMMA[a]	3	18.9	9.0	2.1
PMMA[a]	4	20.7	8.6	2.4
PMMA[a]	5	21.0	6.8	3.1
PMMA[a]	6	19.9	7.4	2.7
PMMA[b]	0.25	25.0	9.6	2.6
PS[a]	1	6.0	2.7	2.2
PS[a]	2	9.0	3.2	2.8
PS[a]	3	12.0	3.4	3.5
PS[a]	4	16.4	3.7	4.4
PS[a]	5	19.0	4.0	4.7
PS[a]	6	21.9	4.1	5.3
PS[b]	1	0.9	0.5	1.8
PS[b]	2	19.3	6.2	3.1
PS[c]	1	28.3	10.5	2.7
PS[c]	6	68.3	20.1	3.4

[a]Polymerization reactions were conducted under 360 nm nominal light irradiation in solution using DCM as solvent.
[b]Polymerization reactions were conducted under 360 nm nominal light irradiation in bulk condition.
[c]Polymerization reactions were conducted under 360 nm using ethyl acetate as solvent.
[d]Determined by GPC.

chromatography (GPC) analysis showed weight average molecular weights (M_w) of up to 68.3 kDa for polystyrene and 21 kDa for poly(methyl methacrylate) (PMMA). As anticipated, longer polymerization times led to increased conversions and broader dispersity index for both polymers (Supplementary Table S1). Gel permeation chromatography (GPC) analysis revealed the emergence of bimodal distributions in the chromatograms of samples subjected to extended reaction times (Supplementary Figure S1). This bimodal behavior is likely attributed to coupling and disproportionation reactions occurring during the termination step of free-radical polymerization. Prior to the formation of the bimodal molecular

weight distribution, a slight decrease in dispersity was observed, suggesting a reduction in the population of oligomers within the reaction medium.

In addition to GPC, ^{1}H-NMR spectra (Supplementary Figure S2) of the photochemically synthesized PMMA and PS can be found in the supporting information.

Control experiments conducted without phenacyl bromide (PAB) showed no monomer conversion, indicating PAB's crucial role as a photoinitiator.

In addition to control experiments, S and MMA polymerization, we conducted PhotoDSC to evaluate the photoinitiation efficiency
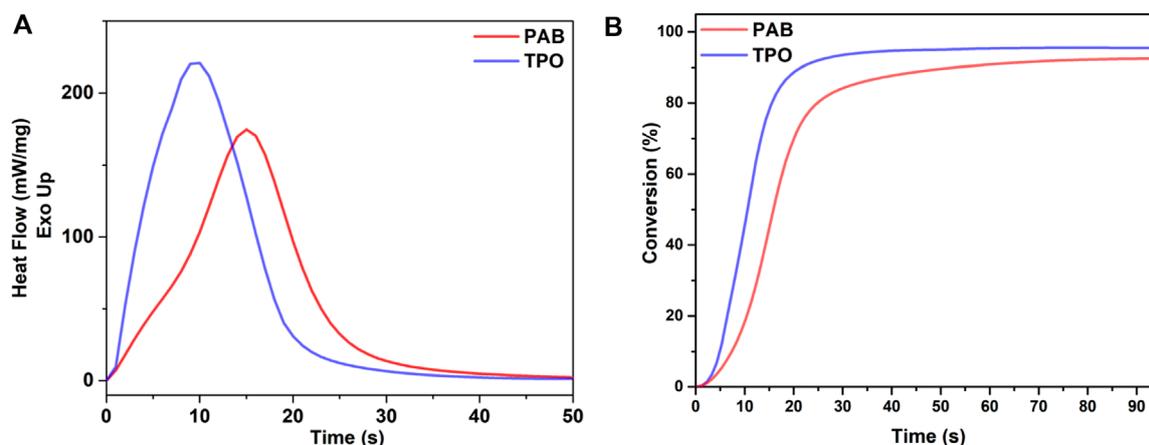
FIGURE 2
(A) Heat flow versus irradiation time graph of the polymerizations of TEGDMA monomer using PAB under 100 mW cm^{-1} irradiation. **(B)** Conversion versus irradiation time graph of the polymerizations of TEGDMA monomer using PAB under 100 mW cm^{-1} irradiation.
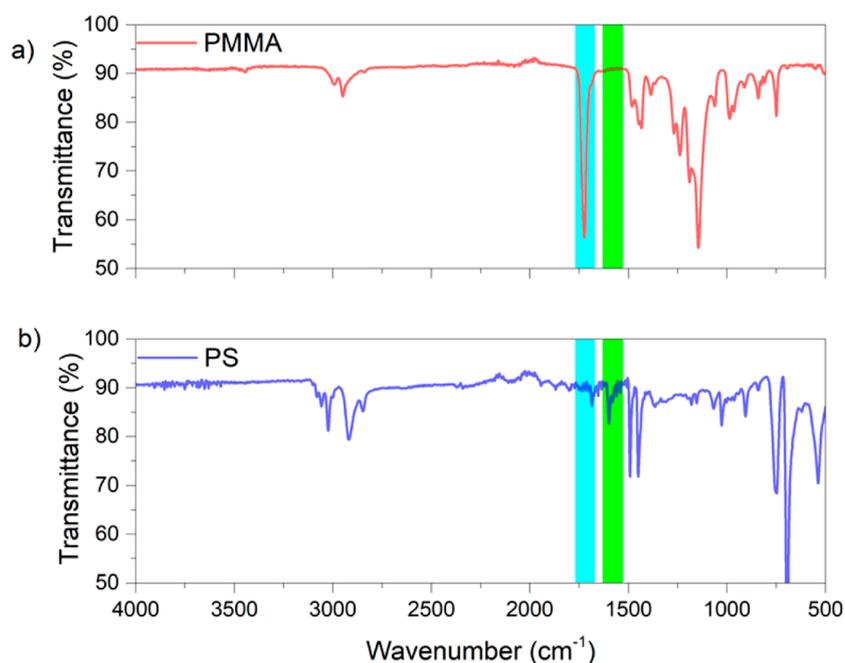
FIGURE 3
FTIR spectra of **(A)**PMMA, **(B)**PS initiated via PAB.

of PAB. Since, photo DSC is a powerful and accurate technique for real-time monitoring of monomer conversions. We compared PAB's performance in the radical polymerization of triethylene glycol dimethacrylate (TEGDMA), a classical di-functional acrylate, with that of diphenyl(2,4,6-trimethylbenzoyl)phosphine oxide (TPO), a commercial and highly efficient photoinitiator commonly used in 3D printing applications.

Figure 2A illustrates the photocuring exotherms of TEGDMA in the presence of PAB and TPO using polychromatic irradiation (λ = 320–500 nm). Figure 2B shows the percentage conversion of TEGDMA over time for both photoinitiators. Although PAB's photoinitiation efficiency is slightly lower than TPO's, it remains comparable. Considering the previously demonstrated advantages of PAB, (Kaya, 2023; Tabak et al., 2024b; Tabak et al., 2024a) including its ability to produce chain-end functional polymers, these PhotoDSC results suggest that PAB could serve as a promising alternative to TPO in various 3D printing applications, especially where post polymer modification and/or chain extension is required for further usage.

In order to characterize the presence of acetophenone radical-initiated polystyrene) and poly(methyl methacrylate), Fourier-Transform infrared (FTIR) spectroscopy was used. In the PS spectrum, a carbonyl stretching band around 1,700 cm^{-1} (highlighted in blue) indicated the presence of trace amounts of acetophenone groups. Conversely, the PMMA spectrum showed no evidence of aromatic C–H stretching bands (approximately 3,100 cm^{-1}) or aromatic C=C stretching bands (approximately 1,550 cm^{-1}), which are highlighted in green (Figure 3). This spectral analysis confirms the successful incorporation of the initiator fragments into the polymer chains and provides insight into the initiation mechanism.

One of the primary advantages of PAB is its ability to generate chain-end functional polymers that can be further utilized in the synthesis of a variety of polymers such as block or graft copolymers. This functionality was exploited in this study to synthesize block copolymers via halogen abstraction chemistry. Dimanganese decacarbonyl ($Mn_2(CO)_{10}$) is a well-established reagent known for its photo-cleavability under visible light irradiation. Upon irradiation, $Mn_2(CO)_{10}$ dissociates, forming manganese pentacarbonyl radicals ($\bullet Mn(CO)_5$) capable of abstracting halogens from organohalide structures (Scheme 1C). By integrating the halogen abstraction capability of $Mn_2(CO)_{10}$ with the chain-end bromine-functionalized photochemically synthesized PMMA and PS from PAB, the formation of block copolymers (PMMA-b-PS) can be achieved.

Accordingly, GPC analysis after irradiating bromine end functional PS with $Mn_2(CO)_{10}$ and MMA revealed a significant increase in weight-average molecular weight from M_w = 20 kDa to M_w = 53 kDa. However, the GPC chromatogram exhibited two distinct peaks for both reactions, indicating the presence of unreacted bromine-functional polymers alongside non-reactive acetophenone-functional precursor polymers in the precipitate (Figure 4). Additionally, the observed molecular weight distribution may be influenced by radical coupling reactions associated with the termination step of the polymerization and halogen abstraction process.

To further characterize the block copolymer composition, ^{1}H NMR spectroscopy was employed. The NMR spectra revealed a

FIGURE 4
GPC chromatograms of bromine functional PS macroinitiator and PS-b-PMMA synthesized via $Mn_2(CO)_{10}$.
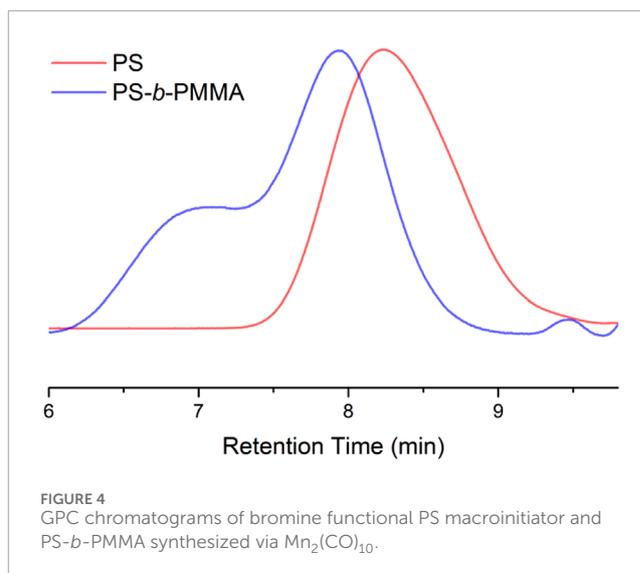
styrene to MMA ratio of 1:1.2 in the block copolymer synthesized using the styrene macroinitiator (Supplementary Figure S3). This ratio provides insight into the relative block lengths and the efficiency of the chain extension process.

4 Conclusion

We have developed a facile radical photopolymerization method utilizing phenacyl bromide as a Type I photoinitiator to produce chain-end bromine functional polymers. These functionalized polymers serve as versatile precursors for the synthesis of various copolymer architectures. The polymerization conditions for this light-induced technique have been optimized through comprehensive analysis of gel permeation chromatography and gravimetric results. The presence of bromine end-functionality was demonstrated through the synthesis of PMMA-PS block copolymers, facilitated by the halogen abstraction capability of $\bullet Mn(CO)_5$ radicals. These results collectively demonstrate the effectiveness of our novel approach in synthesizing bromine end-functional polymers and further block copolymers. Apparently, such photo initiating system can be utilized for the production of a variety of polymers that can be utilized in several applications like additive manufacturing and lithography for the post-functionalization of printed materials to broaden the horizon of the 3D printing applications.

Data availability statement

The original contributions presented in the study are included in the article/Supplementary Material, further inquiries can be directed to the corresponding authors.

Author contributions

MK: Data curation, Investigation, Methodology, Validation, Writing–review and editing. YC: Data curation, Investigation,

Methodology, Validation, Writing–review and editing. KK: Conceptualization, Data curation, Investigation, Writing–original draft. HK: Conceptualization, Data curation, Investigation, Methodology, Software, Validation, Writing–original draft, Writing–review and editing. BK: Funding acquisition, Project administration, Supervision, Writing–original draft, Writing–review and editing.

Funding

Acknowledgments

Conflict of interest

The authors declare that the research was conducted in the absence of any commercial or financial relationships that could be construed as a potential conflict of interest.

Publisher's note

All claims expressed in this article are solely those of the authors and do not necessarily represent those of their affiliated organizations, or those of the publisher, the editors and the reviewers. Any product that may be evaluated in this article, or claim that may be made by its manufacturer, is not guaranteed or endorsed by the publisher.

Supplementary material

The Supplementary Material for this article can be found online at: https://www.frontiersin.org/articles/10.3389/fmats.2024.1490070/full#supplementary-material

References

Albini, A., and Fagnoni, M. (2004). Green chemistry and photochemistry were born at the same time. *Green Chem.* 6, 1–6. doi:10.1039/b309592d

Allushi, A., Kutahya, C., Aydogan, C., Kreutzer, J., Yilmaz, G., and Yagci, Y. (2017). Conventional Type II photoinitiators as activators for photoinduced metal-free atom transfer radical polymerization. *Polym. Chem.* 8, 1972–1977. doi:10.1039/c7py00114b

Andrzejewska, E., and Andrzejewski, M. (1998). Polymerization kinetics of photocurable acrylic resins. *J. Polym. Sci. Part A Polym. Chem.* 36, 665–673. doi:10.1002/(SICI)1099-0518(199803)36:4<665::AID-POLA15>3.0.CO;2-K

Anseth, K. S., Wang, C. M., and Bowman, C. N. (1994a). Kinetic evidence of reaction diffusion during the polymerization of multi(meth)acrylate monomers. *Macromolecules* 27, 650–655. doi:10.1021/ma00081a004

Anseth, K. S., Wang, C. M., and Bowman, C. N. (1994b). Reaction behaviour and kinetic constants for photopolymerizations of multi(meth)acrylate monomers. *Polymer* 35, 3243–3250. doi:10.1016/0032-3861(94)90129-5

Arslan, Z., Kiliclar, H. C., and Yagci, Y. (2022). Dimanganese decacarbonyl catalyzed visible light induced ambient temperature depolymerization of poly(methyl methacrylate). *Des. Monomers Polym.* 25, 271–276. doi:10.1080/15685551.2022.2135730

Aydogan, C., Yilmaz, G., and Yagci, Y. (2017). Synthesis of hyperbranched polymers by photoinduced metal-free ATRP. *Macromolecules* 50, 9115–9120. doi:10.1021/acs.macromol.7b02240

Bobrin, V. A., Yao, Y., Shi, X., Xiu, Y., Zhang, J., Corrigan, N., et al. (2022). Nano-to macro-scale control of 3D printed materials via polymerization induced microphase separation. *Nat. Commun.* 13 (1 13), 3577–3610. doi:10.1038/s41467-022-31095-9

Buchon, L., Becht, J.-M., Rubatat, L., Wang, W., Wei, H., Xiao, P., et al. (2023). Towards safe phosphine oxides photoinitiators with good cytocompatibility for 3D printing of thermoplastics. *J. Appl. Polym. Sci.* 140, e54694. doi:10.1002/app.54694

Cakir, Y. B., Kiliclar, H. C., and Yagci, Y. (2023). Metal free, white LED induced, room temperature degradation of methyl methacrylate - methyl haloacrylate copolymers. *React. Funct. Polym.* 191, 105656. doi:10.1016/j.reactfunctpolym.2023.105656

Ciftci, M., and Yagci, Y. (2018). Block copolymers by mechanistic transformation from PROAD to iniferter process. *Macromol. Rapid Commun.* 39, e1800464–e1800465. doi:10.1002/marc.201800464

Clark, J. H. (2006). Green chemistry: today (and tomorrow). *Green Chem.* 8, 17–21. doi:10.1039/b516637n

Corrigan, N., Yeow, J., Judzewitsch, P., Xu, J., and Boyer, C. (2019). Seeing the light: advancing materials chemistry through photopolymerization. *Angew. Chem. - Int. Ed.* 58, 5170–5189. doi:10.1002/anie.201805473

Crivello, J. V., and Reichmanis, E. (2014). Photopolymer materials and processes for advanced technologies. *Chem. Mater.* 26, 533–548. doi:10.1021/cm402262g

Dickens, S. H., Stansbury, J. W., Choi, K. M., and Floyd, C. J. E. (2003). Photopolymerization kinetics of methacrylate dental resins. *Macromolecules* 36, 6043–6053. doi:10.1021/ma021675k

Dworakowska, S., Lorandi, F., Gorczyński, A., and Matyjaszewski, K. (2022). Toward green atom transfer radical polymerization: current status and future challenges. *Adv. Sci.* 9, 2106076. doi:10.1002/ADVS.202106076

Ghosh, P., Mitra, P. S., and Banerjee, A. N. (1973). Photopolymerization of methyl methacrylate with the use of bromine as photoinitiator. *J. Polym. Sci. Polym. Chem. Ed.* 11, 2021–2030. doi:10.1002/pol.1973.170110821

Gody, G., Barbey, R., Danial, M., and Perrier, S. (2015). Ultrafast RAFT polymerization: multiblock copolymers within minutes. *Polym. Chem.* 6, 1502–1511. doi:10.1039/C4PY01251H

Ishiwari, F., Okabe, G., Ogiwara, H., Kajitani, T., Tokita, M., Takata, M., et al. (2018). Terminal functionalization with a triptycene motif that dramatically changes the structural and physical properties of an amorphous polymer. *J. Am. Chem. Soc.* 140, 13497–13502. doi:10.1021/jacs.8b09242

Kaya, K. (2023). A green and fast method for PEDOT: photoinduced step-growth polymerization of EDOT. *React. Funct. Polym.* 182, 105464. doi:10.1016/J.REACTFUNCTPOLYM.2022.105464

Kaya, K., Cem Kiliclar, H., and Yagci, Y. (2023). Photochemically generated ionic species for cationic and step-growth polymerizations. *Eur. Polym. J.* 112000, 112000. doi:10.1016/J.EURPOLYMJ.2023.112000

Kiliclar, H. C., Yilmaz, G., Li, Z., Zheng, Y., and Yagci, Y. (2022). Photoinduced side-chain functionalization, grafting, cross-linking, and chain extension by thiol-epoxide click reaction using photo base generator. *Macromol. Chem. Phys.* 224, 2200343. doi:10.1002/MACP.202200343

Kowalska, A., Sokolowski, J., and Bociong, K. (2021). The photoinitiators used in resin based dental composite—a review and future perspectives. *Polymers* 13, 470. doi:10.3390/polym13030470

Kumar, D., Mohammad, S. A., Kumar, A., Mane, S. R., and Banerjee, S. (2022). An amino acid-derived ABCBA-type antifouling biohybrid with multi-stimuli responsivity and contaminant removal capability. *Polym. Chem.* 13, 1960–1969. doi:10.1039/D2PY00280A

Lalevée, J., and Fouassier, J. P. (2015). Chapter 8. Recent advances in photoinduced polymerization reactions under 400–700 nm light. *Photochemistry* 42, 215–232. doi:10.1039/9781782624547-00215

Lalevée, J., Mokbel, H., and Fouassier, J. P. (2015). Recent developments of versatile photoinitiating systems for cationic ring opening polymerization operating at any wavelengths and under low light intensity sources. *Molecules* 20, 7201–7221. doi:10.3390/MOLECULES20047201

Matyjaszewski, K., Wang, J. L., Grimaud, T., and Shipp, D. A. (1998). Controlled/"living" atom transfer radical polymerization of methyl methacrylate using various initiation systems. *Macromolecules* 31, 1527–1534. doi:10.1021/ma971298p

Matyjaszewski, K., and Xia, J. (2001). Atom transfer radical polymerization. *Chem. Rev.* 101, 2921–2990. doi:10.1021/cr940534g

McGimpsey, W. G., and Scaiano, J. C. (1988). Photochemistry of α-chloro- and α-bromoacetophenone. Determination of extinction coefficients for halogen–benzene complexes. *Can. J. Chem.* 66, 1474–1478. doi:10.1139/v88-237

Mohammad, S. A., Dolui, S., Kumar, D., Mane, S. R., and Banerjee, S. (2021a). Facile access to functional polyacrylates with dual stimuli response and tunable surface hydrophobicity. *Polym. Chem.* 12, 3042–3051. doi:10.1039/D1PY00378J

Mohammad, S. A., Dolui, S., Kumar, D., Mane, S. R., and Banerjee, S. (2021b). l-Histidine-Derived smart antifouling biohybrid with multistimuli responsivity. *Biomacromolecules* 22, 3941–3949. doi:10.1021/acs.biomac.1c00748

Ober, C. K., Käfer, F., and Yuan, C. (2023). Recent developments in photoresists for extreme-ultraviolet lithography. *Polymer* 280, 126020. doi:10.1016/j.polymer.2023.126020

Ober, M. S., Romer, D. R., Etienne, J., Thomas, P. J., Jain, V., Cameron, J. F., et al. (2019). Backbone degradable poly(aryl acetal) photoresist polymers: synthesis, acid sensitivity, and extreme ultraviolet lithography performance. *Macromolecules* 52, 886–895. doi:10.1021/acs.macromol.8b01038

Otsu, T. (2000). Iniferter concept and living radical polymerization. *J. Polym. Sci. A Polym. Chem.* 38, 2121–2136. doi:10.1002/(SICI)1099-0518(20000615)38:12<2121::AID-POLA10>3.0.CO;2-X

Petko, F., Galek, M., Hola, E., Popielarz, R., and Ortyl, J. (2021). One-component cationic photoinitiators from tunable benzylidene scaffolds for 3D printing applications. *Macromolecules* 54, 7070–7087. doi:10.1021/acs.macromol.1c01048

Petko, F., Galek, M., Hola, E., Topa-Skwarczyńska, M., Tomal, W., Jankowska, M., et al. (2022). Symmetric iodonium salts based on benzylidene as one-component photoinitiators for applications in 3D printing. *Chem. Mater.* 34, 10077–10092. doi:10.1021/acs.chemmater.2c02796

Pispas, S., and Hadjichristidis, N. (1994). End-functionalized block copolymers of styrene and isoprene: synthesis and association behavior in dilute solution. *Macromolecules* 27, 1891–1896. doi:10.1021/ma00085a035

Tabak, T., Altinisik, S., Ulucay, S., Koyuncu, S., and Kaya, K. (2024a). Black-to-Transmissive electrochromic switching PEDOT-co-poly(N-ethylcarbazole) via a sustainable and facile *in situ* photo(co)polymerization method. *Macromolecules* 57, 4769–4781. doi:10.1021/acs.macromol.4c00364

Tabak, T., Kaya, K., Isci, R., Ozturk, T., Yagci, Y., and Kiskan, B. (2024b). Combining step-growth and chain-growth polymerizations in One pot: light-induced fabrication of conductive nanoporous PEDOT-PCL scaffold. *Macromol. Rapid Commun.* 45, 2300455. doi:10.1002/marc.202300455

Tomal, W., Cem Kiliclar, H., Fiedor, P., Ortyl, J., Yagci, Y., Tomal, W., et al. (2022). Visible light induced high resolution and swift 3D printing system by halogen atom transfer. *Macromol. Rapid Commun.* 2200661, e2200661. doi:10.1002/MARC.202200661

Tomal, W., Świergosz, T., Pilch, M., Kasprzyk, W., and Ortyl, J. (2021). New horizons for carbon dots: quantum nano-photoinitiating catalysts for cationic photopolymerization and three-dimensional (3D) printing under visible light. *Polym. Chem.* 12, 3661–3676. doi:10.1039/d1py00228g

Yagci, Y., Jockusch, S., and Turro, N. J. (2010). Photoinitiated polymerization: advances, challenges, and opportunities. *Macromolecules* 43, 6245–6260. doi:10.1021/ma1007545

Yagci, Y., and Tasdelen, M. A. (2006). Mechanistic transformations involving living and controlled/living polymerization methods. *Prog. Polym. Sci. Oxf.* 31, 1133–1170. doi:10.1016/j.progpolymsci.2006.07.003

Zha, R. H., de Waal, B. F. M., Lutz, M., Teunissen, A. J. P., and Meijer, E. W. (2016). End groups of functionalized siloxane oligomers direct block-copolymeric or liquid-crystalline self-assembly behavior. *J. Am. Chem. Soc.* 138, 5693–5698. doi:10.1021/jacs.6b02172

Zhang, Z., Corrigan, N., Bagheri, A., Jin, J., and Boyer, C. (2019). A versatile 3D and 4D printing system through photocontrolled RAFT polymerization. *Angew. Chem.* 131, 18122–18131. doi:10.1002/ange.201912608